Measurement of Loss in Inductors and Transformers in xEV Power Supplies

By Kazunobu Hayashi and Shozo Yoda

HIOKI E.E. Corporation

1. Introduction

Amid efforts to realize a sustainable society, development of technologies for reducing greenhouse gas emissions is proceeding apace. One such initiative is the electrification of automobiles [1] [2].

One serious issue facing electrification–one that affects freedom of design with regard to performance and component shape–is the need to increase the efficiency of power supplies while reducing their size and weight. To resolve this issue, it is necessary to accurately measure and assess loss in the components that make up power supplies. It is particularly important to accurately assess loss and work towards improvements in inductors and transformers, which account for a large proportion of power supplies' volume, weight, and loss [3] That said, accurate measurement is made difficult by the fact that these devices operate at low power factors, with the phase difference between their voltage and current at close to 90°, and that the frequencies they use are increasing as semiconductor devices continue to evolve [4] [5].

This article introduces expertise, measurement results, and other information related to measurement of loss in inductors and transformers used in power supplies for xEVs.

2. Types of power supplies in xEVs and associated issues

Types of power supplies

Various types of power supplies (power converters) are used in xEVs. Fig. 1 provides a conceptual diagram for a power supply used in a battery electric vehicle (BEV). An onboard charger (OBC) or rapid charger is used to charge the vehicle's battery. Such chargers incorporate an AC/DC converter that converts grid power to the battery's high DC voltage. Thanks to mechanisms like vehicle-to-home (V2H) and vehicle-to-grid (V2G), which are designed to allow power from vehicle batteries to be used at homes and on the power grid, the industry is increasingly adopting vehicle chargers that can supply power in both directions. Step-up DC/DC converters and inverters are used in powertrains. A DC/DC converter is used to combine power from the main battery and an auxiliary 12 V battery. Power electronics technologies are being used to make these power supplies smaller and lighter while boosting their efficiency.

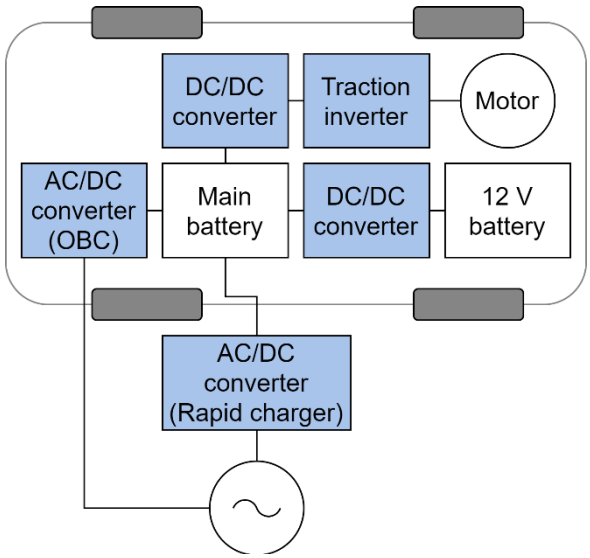

Fig. 1 Example of power supply architecture in a BEV

Issues in power supply development

For example, one key issue in the development of BEVs is the need to increase range by improving energy efficiency [6]. Since batteries have lower energy density than fossil fuels [7], BEVs must be equipped with high-capacity batteries in order to deliver range on par with that of vehicles powered by an internal combustion engine. Doing so drives up vehicle costs, and the associated increase in weight worsens energy efficiency; as a result, manufacturers are under pressure to realize increased range by equipping their vehicles with smaller batteries.

To increase range with batteries of the same or smaller size, it is necessary to improve energy efficiency by designing more efficient, lightweight, and compact power supplies. Loss in power supplies can be reduced by boosting efficiency. More lightweight designs make possible vehicles that weigh less overall and that have lower driving loss. Furthermore, more compact power supplies increase the degree of freedom with which components can be placed in vehicles while helping reduce vehicle Cd values and increasing occupant comfort.

In this way, increasing efficiency while reducing weight and size are issues in the development of xEV power supplies.

Inductors and transformers

Many vehicle power supplies employ switching circuits that use semiconductor switches in order to increase efficiency while reducing weight and size. Most switching circuits incorporate inductors (reactors) and transformers. Since inductors and transformers consist of a magnetic core fabricated primarily from iron and copper wires, they are known to account for a large proportion of power supplies' volume and weight [3]. Furthermore, widespread adoption of wide-bandgap (WBG) semiconductors made from materials like SiC and GaN is making possible higher switching frequencies and lower-loss semiconductors, facilitating smaller, lighter, lower-loss power supplies and increasing the impact of inductors and transformers on overall power supply performance.

Against this backdrop, increasing the performance of power supplies–in other words, of inductors and transformers–is becoming a key priority in the drive to increase xEV performance. Consequently, manufacturers need to assess and reduce loss in inductors and transformers.

3. Methods for measuring loss in inductors and transformers

Measurement of overall circuit loss

When evaluating inductors and transformers, the relationship between the circuit's operating conditions and inductor/transformer loss can be understood by measuring overall loss in the circuit containing the components. Fig. 2 illustrates an example connection in which overall circuit efficiency (loss) is measured for a non-isolated boost chopper DC/DC converter. The circuit's overall loss (Equation (1)) and efficiency (Equation (2)) can be calculated by measuring input and output DC power and then calculating their difference and ratio.

$$P_{\text{loss}} = P_1 - P_2 \quad (1)$$

$$\eta = \frac{P_2}{P_1} \cdot 100\ [\%] \quad (2)$$

Since power analyzers like the PW8001 come programmed with the measurement parameters needed to measure loss and efficiency, it is possible to calculate loss and efficiency automatically simply by configuring the instrument with the input and output power measurement channels.

In most cases, the circuit's overall input and output power will be either DC power or power at the grid frequency. Consequently, if you wish to measure a circuit's loss and efficiency with a high degree of precision, it is important to choose a power analyzer and current sensors with high accuracy at DC and grid frequencies.

When measuring loss based on the difference between input and output, it is important to synchronize the timing at which measurements are made. Loss values are particularly susceptible to the effects of differences in the timing of input and output measurements made while the condition of the measurement target is fluctuating, for example due to transient states. Power analyzers allow the user to set measurement timing by selecting a synchronization source. In the case of Fig. 2, the input and output are both DC, so using DC as the synchronization source allows input and output measurements to be timed using the data refresh rate determined by the instrument's internal clock. If the input and output include AC signals, as in Fig. 5, stable loss measurement can generally be accomplished by using the AC measurement channel with the slowest frequency as the synchronization source. In the case of Fig. 5, it is desirable to set the synchronization source for all channels to CH1 (input grid power).

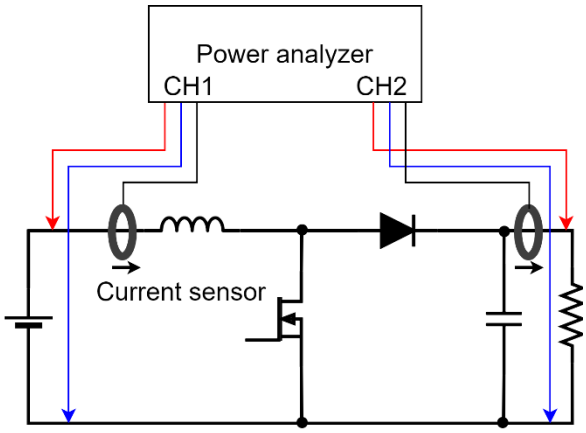

Fig. 2 Connection diagram for measuring overall loss in a boost chopper circuit

Measurement of inductor loss

Inductor loss can be measured by using a power analyzer and current sensor to measure the voltage across the inductor's terminals and the current flowing through the device. Fig. 3 illustrates example connections for measuring inductor loss in a non-isolated step-down chopper DC/DC converter. In a step-down chopper, connecting the current sensor to the output side of the inductor being measured yields more stable measurement results. Since the voltage value at an inductor's input-side node varies with each switching cycle, the voltage waveform will include high-frequency components. By contrast, voltage fluctuations at an inductor's output-side node are less pronounced due to the DC voltage found there. In general, connecting the current sensor to the output side, where there are fewer high-frequency components, yields more stable results since sensors' common-mode rejection ratio (CMRR) decreases at high frequencies.

In addition, in order to realize high-precision loss measurement, it is necessary to use a power analyzer and current sensors that provide high phase precision and noise resistance at the circuit's switching frequency and its harmonic components.

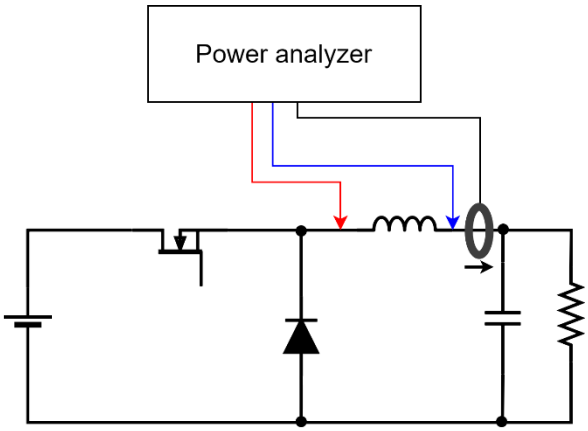

Fig. 3 Connection diagram for measuring loss in the inductor of a step-down chopper circuit

Measurement of transformer loss

As when measuring overall loss in a circuit, transformer loss can be measured by measuring the input and output power for the transformer being measured and then calculating the difference. As an example, Fig. 4 illustrates connections for measuring loss in an isolated full-bridge DC/DC converter's transformer. If the transformer has multiple output circuits, it is necessary to measure power for all output circuits. Using a power analyzer's efficiency measurement function, the loss and efficiency for the setup shown in Fig. 4 can be calculated using Equations (1) and (2). Transformer output takes the form of an AC signal that includes the switching frequency and its harmonic components. In addition, the effects of factors including excitation current result in a comparatively low power factor. Consequently, it is necessary to use a power analyzer and current sensor with sufficient gain precision and phase precision at the switching frequency and its harmonic components.

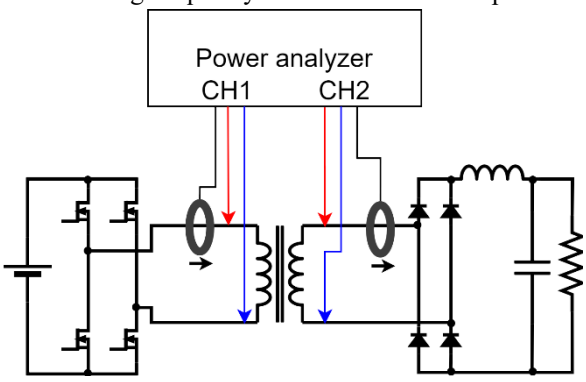

Fig. 4 Connection diagram for measuring loss in the transformer of an isolated full-bridge DC/DC converter

Example connections (OBC)

Fig. 5 illustrates example connections for measuring loss in an xEV onboard charger (OBC). The typical OBC uses a power factor correction (PFC) circuit to convert input grid power to high-voltage DC power

and an isolated DC/DC converter to adjust the voltage value before supplying DC power to the battery to charge it. Equation (3) can be used to calculate overall loss in the OBC; Equation (4), loss in the PFC inductor; Equation (5), loss in the PFC circuit; Equation (6), loss in the isolated DC/DC converter's transformer; and Equation (7), loss in the isolated DC/DC converter.

$$P_{\mathrm{ALL}} = P_1 - P_6 \quad (3)$$

$$P_{\mathrm{L\,PFC}} = P_2 \quad (4)$$

$$P_{\mathrm{PFC}} = P_1 - P_3 \quad (5)$$

$$P_{\mathrm{trans}} = P_4 - P_5 \quad (6)$$

$$P_{\mathrm{DC/DC}} = P_3 - P_6 \quad (7)$$

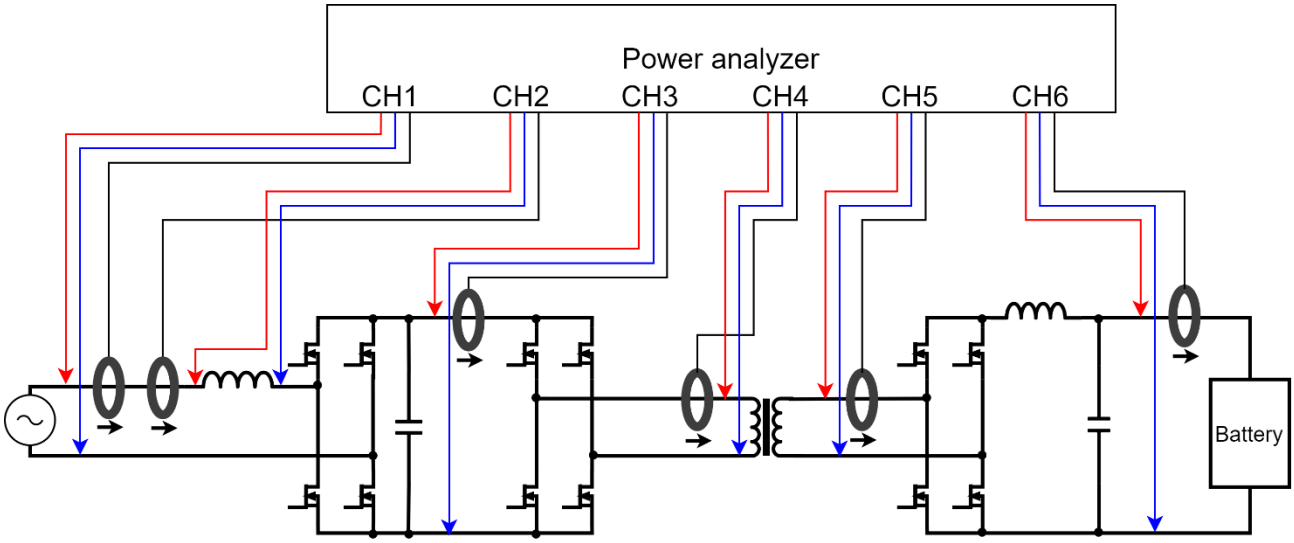

Fig. 5 Connection diagram for measuring loss in the components of an onboard charger

4. Instrument performance needed to measure inductors and transformers

Phase characteristics

The phase difference between the voltage and current applied to inductors approaches 90°, with the result that the measuring instrument's phase error has a significant effect on error in power loss measurement [4]. If the measurement target's phase difference is given by θ and the instrument's phase error by $\Delta\theta$, the loss measurement error rate k can be expressed as shown in Equation (8).

$$k = \frac{\cos(\theta + \Delta\theta) - \cos\theta}{\cos\theta} \cdot 100\ [\%] \quad (8)$$

Fig. 6 illustrates the relationship between loss and the phase difference between the measurement target's voltage and current. For example, if the measurement target's phase difference is 89° and the instrument's phase error is ±0.1°, the loss measurement error will be ±10%. In this way, an instrument with low phase error at the circuit's switching frequency and its harmonic frequencies should be used to measure loss in inductors and transformers.

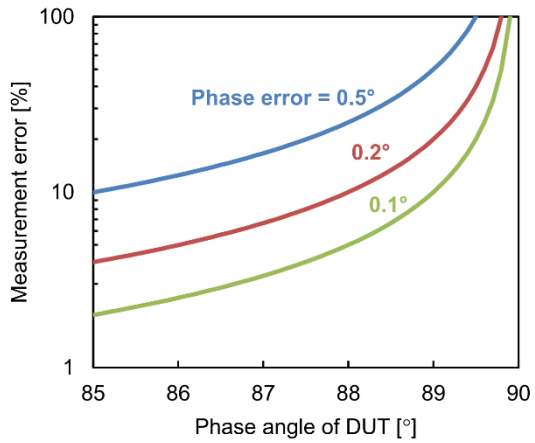

Fig. 6 Influence of instrument phase error on active power

DC accuracy

A DC currents is superposed in the inductors of boost chopper circuits and step-down chopper circuits due to the circuit load current. This DC current and the inductor's winding resistance result in DC loss. Since the instrument's DC accuracy becomes an important consideration when measuring loss in an inductor such as these, it is necessary to use an instrument with high DC accuracy. In addition, power analyzers and current sensors inevitably exhibit fluctuations in offset error due to temperature and changes over time, and these offset errors affect DC loss measurement results. To eliminate these effects so that more accurate measurement can be achieved, the instrument's zero adjustment function should be used prior to measurement to eliminate offset error.

The test results described in this paper were obtained using Hioki's flux-gate current sensors. These sensors are distinguished by their minimization of the effects of sensor core magnetization due to the measurement current and of the effects of conductor position inside the current sensor [8] [9]. Consequently, they can be used with peace of mind to evaluate DC loss on the order of 1% or less, and they are widely used in WLTP energy efficiency evaluation by OEM manufacturers.

Large-current measurement

Most power supplies being developed for use in xEVs are characterized by measurement targets to which large currents flow, making it difficult to make measurements using typical shunt resistors. In that approach, low-resistance shunt resistors must be used in order to reduce power loss in the shunt resistor. Disadvantages of this approach include an inevitable deterioration of frequency characteristics due to factors such as parasitic inductance, and decreased reproducibility due to measured value drift caused by heating of the shunt resistor. Consequently, it is recommended to make measurements using current sensors.

Current sensors' phase delay poses a problem. For the typical current sensor, phase delay becomes noteworthy above 10 kHz. As a result, it is necessary to ascertain the phase characteristics of the current sensors being used and to have the power analyzer accurately correct those characteristics during measurement.

The test results described in this paper were obtained after correcting phase error occurring due to the time delay between the current sensors' input and output using the automatic phase correction function available when the Power Analyzer PW8001 is combined with Hioki current sensors. Current sensors that support the automatic phase correction function store phase calibration results obtained at the time of shipment in their internal memory. The PW8001 reads this data and uses it to automatically correct phase error during measurement. In this way, low-phase-error power measurement can be carried out across a broad measurement band.

Current sensors have a disadvantage in the effects of conductor position. This phenomenon is characterized by variations in measured values when the conductor under measurement is moved about within the hole in the current sensor. These effects can degrade the reproducibility of measured values and make it impossible to obtain reliable measurement results. They tend to become more pronounced as the frequency of the current being measured increases. Thanks to its innovative winding and shielding, the CT6904A is less susceptible to the effects of conductor position, allowing the sensor to deliver high reproducibility when measuring loss in high-frequency inductors and transformers [8] [9]. Fig. 7 provides a comparison of the effects of conductor position on phase at 100 kHz between the CT6904A and a competitor's pass-through sensor. The graph makes

clear that these effects are limited to 1/10 to 1/100 or less compared to the competing sensor.

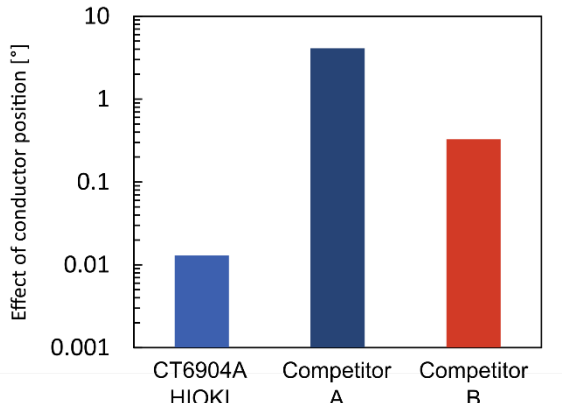

Fig. 7 Effects of conductor position on phase characteristics in high-accuracy, pass-through type current sensors at 100 kHz

Noise resistance

The increase in switching frequencies being driven by WBG semiconductors poses the problem of increased effects of electromagnetic noise. Such effects must be reduced as they can impact electrical measurements. Together, Hioki's PW8001 and CT6904A deliver a CMRR of at least 110 dB/100 kHz. This level of performance makes it possible to obtain stable measured values without being affected by noise.

5. Example measurement of inductor loss

Evaluation of power analyzer and current sensor characteristics when measuring an air-core inductor

To verify the characteristics of a Hioki power analyzer and current sensor, we measured loss when applying a sine wave current to an air-core inductor. Because inductors that use magnetic cores exhibit magnetic core loss level dependency and temperature characteristics, it is extremely difficult to obtain true values for loss. By contrast, air-core inductors, which lack magnetic cores, do not exhibit impedance level dependency. As a result, the equivalent series resistance R_s for a small signal can be measured using a high-precision LCR meter (with accuracy of ±0.05% from 20 Hz to 2 MHz), and the the air-inductor's loss $P_{\text{air core}}$ can be calculated from the resulting value and the current RMS value I_{rms} applied to the air-core inductor using the following equation, providing a standard that can be used to evaluate power analyzer characteristics:

$$P_{\text{air core}} = I_{\text{rms}}^2 \cdot R_s \qquad (9)$$

We used the Power Analyzer PW8001 and the U7005 (±0.03% accuracy, 5 MHz band) as its measurement unit. The CT6904A (±0.027% accuracy, 4 MHz band) was used as the current sensor. Using the measurement circuit illustrated in Fig. 8, we measured loss when a 5 Arms current was applied to the air-core inductor by a power amplifier and compared the loss values calculated using Equation (9). Since the power amplifier could not generate 5 Arms at or above 200 kHz, we conducted the test using a lower current value at those frequencies. The air-core inductor used in the test had an inductance of approximately 11 µH. An ABS resin core fabricated using a 3D printer was used as the non-magnetic core.

Fig. 9 illustrates the test results. It also illustrates the results of making simultaneous measurements with competitor Power Analyzer A (±0.025% accuracy, 10 MHz band) and a pass-through current sensor (200 A rating, ±0.01% accuracy, 1 MHz band). Measurement results are shown for 10 kHz to 100 kHz, the frequency range within which the power amplifier can apply 5 Arms. The results from measurements made with the PW8001 closely track the values calculated from the equivalent series resistance values and RMS current values measured with the LCR meter, indicating that the PW8001 and CT6904A can measure inductor loss over a broader band. By contrast, the measurement results obtained using competing Power Analyzer A diverge significantly from values calculated from equivalent series resistance values at and beyond 20 kHz, indicating that the setup is incapable of accurate loss measurement. Fig. 10 presents the results of measuring the phase angle between the voltage and current applied to the air-core inductor. Using measured values from the power analyzer, the power phase angle was calculated from the active power $P_{\text{air core}}$ and RMS voltage and current values U_{rms}, I_{rms} using Equation (10).

$$\theta = \cos^{-1} \frac{P_{\text{air core}}}{U_{\text{rms}} \cdot I_{\text{rms}}} \qquad (10)$$

For comparison purposes, the same figure also plots the impedance phase angle as measured using the LCR meter. The measurement results from the PW8001 closely track those of the LCR meter, indicating that the former has excellent phase characteristics at high frequencies. Thanks to these excellent phase characteristics, the instrument can measure loss in high-frequency, low-power-factor inductors with a high degree of precision, as shown in Fig. 9.

When the PW8001 is used with the CT6904A, users can choose a maximum range of 1500 V/500 A. This setting can be used to measure loss in operating inductors in high-power circuits. Additionally, the CT6904A's excellent linearity makes possible accurate loss measurement in targets with current values on the order of several amps.

The CT6904A is a current sensor that uses zero-flux operation. As a result, the device does not exhibit magnetic saturation or changes in characteristics since the magnetic field applied to its magnetic core is extremely limited, even if a DC current is superposed on the measurement current. Consequently, the sensor can accurately measure inductor loss under operating conditions in which a DC current is superposed on the inductor, as is typical with DC/DC converters, since its characteristics do not change.

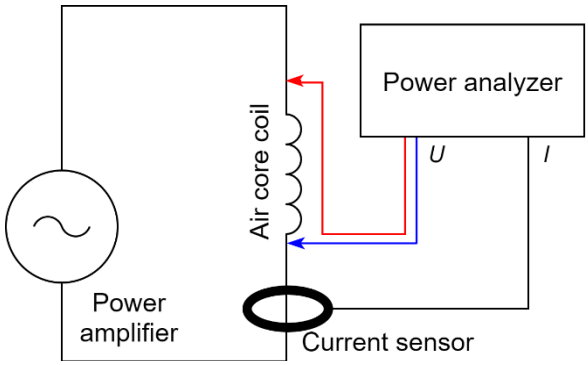

Fig. 8 Test circuit for verifying power analyzer and current sensor characteristics

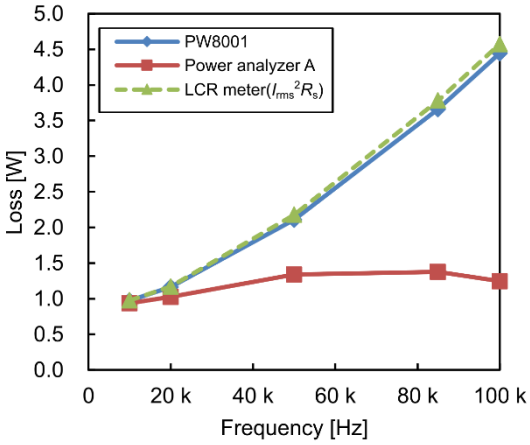

Fig. 9 Loss measurements for an air-core inductor

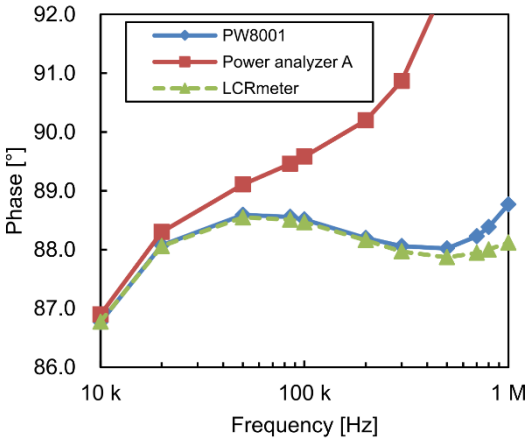

Fig. 10 Phase angle measurements for an air-core inductor

Measurement results for inductor loss in a PFC circuit

We measured loss in an inductor in a power factor correction (PFC) circuit using the two power analyzers whose phase characteristics at high frequencies were evaluated on the previous page (see Fig. 11 for a wiring diagram). Fig. 12 illustrates the results. Loss in an input inductor in a totem pole PFC circuit (Table 1) was measured using a pair of power analyzers. The figure plots inductor loss values obtained after setting the power analyzers' refresh rate to 50 ms and varying the electronic load setting in increments of 100 W. The figure indicates the PW8001 yielded extremely stable results characterized by little variability. By contrast, results obtained from Power Analyzer A exhibit a high level of variability, and the instrument yielded negative inductor loss values in the domain where the circuit's output power was low.

Fig. 10 shows a phase error of approximately +1° for Power Analyzer A at the PFC circuit's switching frequency of 72 kHz. In short, the measured phase exceeded 90° when the measurement target's phase difference was 89° or greater, causing the loss value to appear to be negative. In this way, it is likely that Power Analyzer A's phase error caused the loss value to be measured as a negative value.

Fig. 13 illustrates the operating waveforms for the PFC circuit at an output power of 2 kW. Voltage and current waveforms are provided at three locations: input AC, the inductor, and output DC. In the inductor's voltage and current waveforms, the 72 kHz switching frequency component is superposed on the input frequency's 60 Hz component. This fact likely accounts for the large difference in the extent of variability in the loss values obtained from the PW8001 and Power Analyzer A. In order to measure loss in such waveforms in a stable manner, it is necessary to determine the power calculation interval based on accurate zero-cross detection. The PW8001 achieves accurate, stable zero-cross detection, including for distorted waveforms such as those associated with PWM, by applying digital signal processing to the detection process. In addition, the voltage includes a high-frequency component because it takes the shape of a rectangular wave. As a result, if power calculations are performed without applying an appropriate antialiasing filter, aliasing (folding noise) can cause the appearance of increased variability. Because it was designed to provide an analog measurement band of 10 MHz and a low sampling frequency of about 1 MS/s, Power Analyzer A is susceptible to aliasing. By contrast, the PW8001 (U7005) exhibits no increase in variability due to aliasing because it pairs a 5 MHz analog measurement band with a sampling frequency of 15 MS/s.

In this way, the PW8001 can accomplish accurate, stable measurement of inductor loss in a PFC circuit–ordinarily an extremely difficult task–thanks to its excellent phase characteristics and those of dedicated current sensors at high frequencies, its use of high-speed sampling and an antialiasing filter, and its use of advanced zero-cross detection that leverages digital signal processing.

Table 1 Specifications of the PFC circuit

Board number	STEVAL-DPSTPFC1
Manufacturer	STMicroelectronics
Circuit topology	Bridgeless totem pole PFC
Switching frequency	72 kHz
Switching elements	SiC-MOSFET

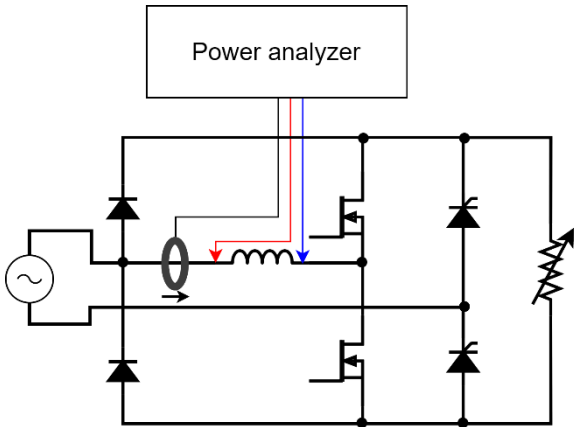

Fig. 11 Test circuit for measuring loss in the inductor in a PFC circuit

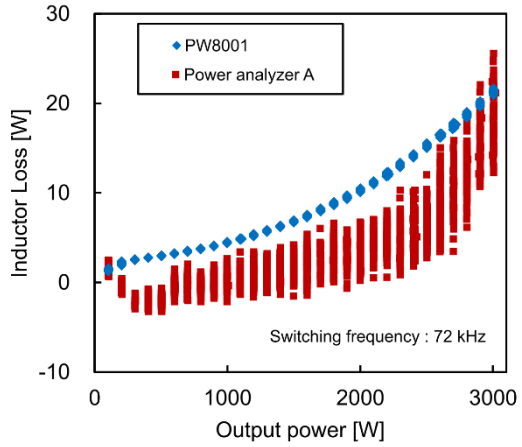

Fig. 12 Loss measurements for the inductor in a PFC circuit

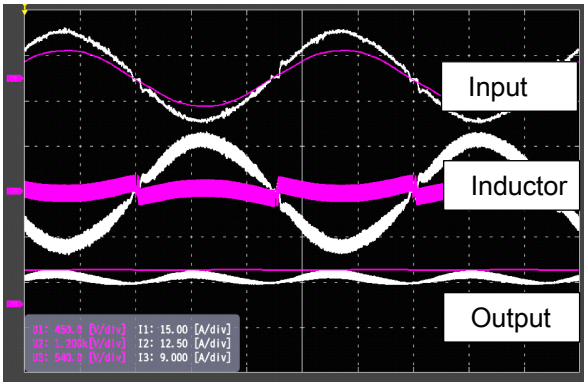

Fig. 13 Waveforms in the PFC circuit

6. Summary

Two serious issues in the electrification of automobiles are increasing power supply efficiency and decreasing power supply size. To address these issues, it is critical to accurately assess loss in inductors and transformers. Because such measurements of loss in inductors and transformers entail measuring low-power-factor power at high frequencies, instruments must provide a high level of performance.

This article has introduced expertise, measurement results, and other information related to measurement of loss in inductors and transformers used in power supplies for xEVs. It demonstrates how the Power Analyzer PW8001 and AC/DC Current Sensor CT6904A can be used to measure inductor and transformer loss with a high degree of precision.

References

[1] M. Okamura and T. Takaoka. “The Evolution of Electric Components in the Prius,” *IEEJ Journal of Industry Applications*, Vol. 11, No. 1, pp.1-6 (2022).

[2] K. Yoshimoto and T. Hanyu. “NISSAN e-POWER: 100% Electric Drive and Powertrain Control,” *IEEJ Journal of Industry Applications*, Vol. 10, No. 4, pp.411-416 (2021).

[3] H. Akagi et. al. “Power-Loss Breakdown of a 750-V 100-kW 20-kHz Bidirectional Isolated DC-DC Converter Using SiC-MOSFET/SBD Dual Modules,” *IEEE Transactions on Industry Applications*, [4] Vol. 51, No. 1, pp. 420-428 (Jan. /Feb. 2015).

[4] H. Matsumori, T. Shimizu, K. Takano, and H. Ishii. “Evaluation of Iron Loss of AC Filter Inductor Used in Three-Phase PWM Inverters Based on an Iron Loss Analyzer,” *IEEE Transactions on Power Electronics*, Vol. 31, No. 4 (2016).

[5] K. Hayashi. “Measurement of Loss in High-Frequency Reactors,” *Bodo’s Power Systems*, pp.18-22 (Feb. 2017).

[6] E. Ishii and M. Yoshida. “Electric Vehicle Simulator for Evaluating Dynamic Energy Performance of Drive Systems with High Accuracy,” *Toshiba Review*, Vol. 67, No. 7 (2022).

[7] H. Nishimoto. “Rechargeable Batteries for Electric Vehicles,” *Tokugikon*, Vol. 274 (2014).

[8] H. Yoda. “AC/DC Current Sensor CT6904/CT6904-60,” *HIOKI Technical Notes* (2019).

[9] M. Harano, H. Yoda, K. Seki, K. Hayashi, T. Komiyama, and S. Yamada. “Development of a Wideband High-Precision Current Sensor for Next Generation Power Electronics Applications,” *Proc. IEEE ECCE*, pp. 3565-3571 (2018).